Supplementary information

Structural analysis of initial lithiation of NiO thin film electrodes

Guennadi Evmenenko,[a] Timothy T. Fister,[b] Fernando C. Castro,[a] Xinqi Chen,[c,d] Byeongdu Lee,[e] D. Bruce Buchholz,[a] Vinayak P. Dravid,[a] Paul Fenter,[b] Michael J. Bedzyk[a,f,*]

[a] *Department of Materials Science and Engineering, Northwestern University, Evanston, Illinois 60208, USA*

[b] *Chemical Sciences and Engineering Division, Argonne National Laboratory, Lemont, Illinois 60439, USA*

[c] *NUANCE Center, Northwestern University, Evanston, Illinois 60208, USA*

[d] *Department of Mechanical Engineering, Northwestern University, Evanston, Illinois 60208, USA*

[e] *X-ray Science Division, Argonne National Laboratory, Lemont, Illinois 60439, USA*

[f] *Department of Physics and Astronomy, Northwestern University, Evanston, Illinois 60208, USA*

* Corresponding author: bedzyk@northwestern.edu

Associated content:

Schematic illustration of pristine bilayer Ni/NiO film and experimental setup with the transmission geometry spectroelectrochemical cell used for *operando* XRR and GISAXS measurements; tabulated mass density, calculated electron density, and critical momentum transfer values of assumed components of the Ni/NiO electrode; the parameters used in the profiles obtained by the best fits of X-ray reflectivity (XRR) data; the first discharge voltammograms for Ni (49.3 Å) / NiO (67.0 Å) and Ni (49.4 Å) / NiO (19.0 Å) electrodes (*operando* XRR and GISAXS measurements); calculated penetration depth of X-rays at photon energy of E = 14.00 keV into NiO film immersed in electrolyte as a function of incident angle α.; Guinier plots of horizontal line cuts of 2D GISAXS patterns at different incident angles for the bilayer Ni (50 Å) / NiO (200 Å) electrode during lithiation; F1s spectra for the Ni (34 Å) / NiO (65 Å) bilayer electrode after the first discharge of the as-deposited film from the open circuit potential (OC) (3.3 V) to 1.7 V at different depth positions; ToF-SIMS depth profiles of Li, Ni and Al for the Ni (34 Å) / NiO (65 Å) bilayer film electrode after discharging the as-deposited film from the OC potential (3.3 V) to 1.7 V; ToF-SIMS depth profiles for pristine Ni (34 Å) / NiO (65 Å) bilayer film spin-coated by PMMA (MW = 495 000) and comparison of Ni depth profiles for pristine (with PMMA on the top) film and lithiated Ni/NiO bilayer film; high-angle annular dark-field (HAADF) STEM image of the lithiated Ni/NiO bilayer cross-section and integrated EELS spectra of the different film layer regions.

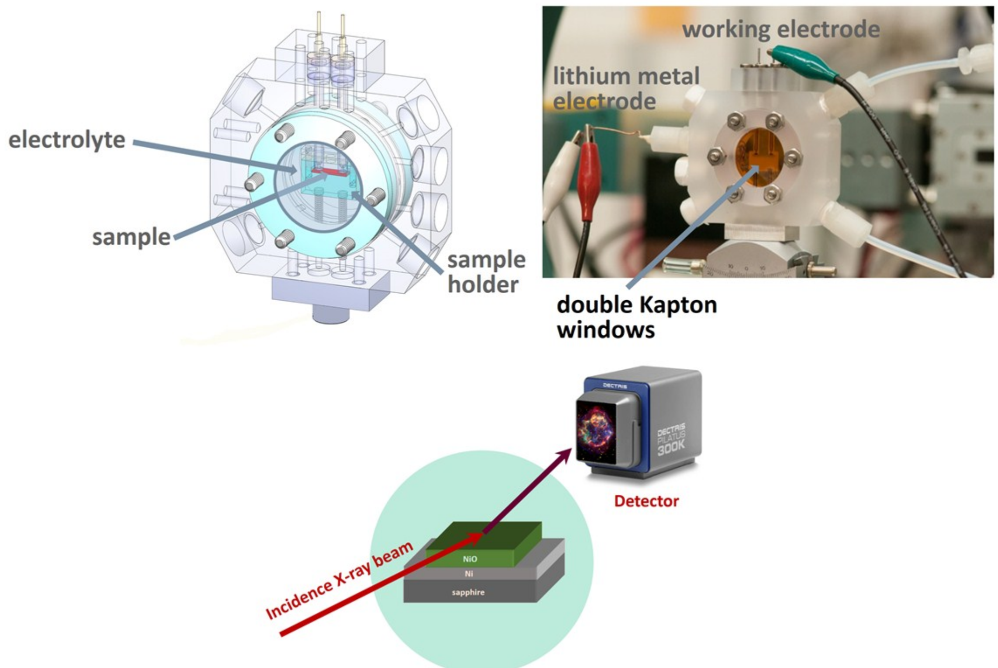

Schematic illustration of pristine bilayer Ni/NiO film and experimental setup with the transmission geometry spectroelectrochemical cell used for *operando* XRR and GISAXS measurements.

Table S1. Tabulated mass densities (ρ) and calculated electron densities (ρ_e) of assumed components of the Ni/NiO electrode.

Compound	Density ρ (g/cm^3)	Effective electron density at 20 keV ρ_e (e$^-$Å^{-3})*	Effective electron density at 8.04 keV ρ_e (e$^-$Å^{-3})*
1 M $LiPF_6$ EC/DMC (1:1 v/v)	1.2	0.38	0.38
NiO	6.67	1.97	1.78
Ni	8.90	2.61	2.28
Li_2O	2.01	0.57	0.57
sapphire	3.97	1.18	1.19

*The electron density, ρ_e, of each layer was calculated from the atomic composition of the compound according to the relationship: $\rho_e = \sum_i (Z_i - \Delta f_i') \cdot \rho \cdot N_A / M$. Here Z_i is the number of electrons in the i^{th} atom, $\Delta f_i'$ is the real part of the anomalous dispersion correction. The summation is carried out over all atoms in the molecular formula for the compound. N_A is Avogadro's number, M is the molecular mass of the compound, and ρ is the mass density of the compound.

Tables of X-ray reflectivity (XRR) fit parameters

The parameters determined from best fits to XRR data of Fig. 1A and used in Fig. 1B for the Ni (49.3 Å) / NiO (67.0 Å) bilayer film are given in Tables S2a-g.

Table S2a. E = 3.25 V (open circuit conditions)

Layer relative to surface	Thickness (Å)	Electron density ρ_e (e^-Å^{-3})	Roughness (Å)
Electrolyte	-	0.38	-
1	67.0	1.97	2.4
2	49.3	2.61	1.7
Substrate	-	1.19	1.5

Table S2b. E = 2.15 V

Layer relative to surface	Thickness (Å)	Electron density ρ_e (e^-Å^{-3})	Roughness (Å)
Electrolyte	-	0.38	-
1	4.2	1.30	1.7
2	16.6	1.94	3.0
3	42.2	1.97	2.0
4	3.8	1.83	2.1
5	49.4	2.61	2.1
Substrate	-	1.19	1.5

Table S2c. E = 1.71 V

Layer relative to surface	Thickness (Å)	Electron density ρ_e (e^{-}Å^{-3})	Roughness (Å)
Electrolyte	-	0.38	-
1	6.4	1.49	2.1
2	14.5	1.93	3.0
3	40.5	1.97	2.0
4	4.3	1.82	2.1
5	49.4	2.61	2.1
Substrate	-	1.19	1.5

Table S2d. E = 1.26 V

Layer relative to surface	Thickness (Å)	Electron density ρ_e (e^{-}Å^{-3})	Roughness (Å)
Electrolyte	-	0.38	-
1	3.9	0.98	1.1
2	5.6	1.57	3.0
3	51.9	1.97	9.8
4	2.7	1.33	2.1
5	50.7	2.61	3.1
Substrate	-	1.19	1.5

Table S2e. E = 0.67 V

Layer relative to surface	Thickness (Å)	Electron density ρ_e ($e^{-}Å^{-3}$)	Roughness (Å)
Electrolyte	-	0.38	-
1	58.0	0.87	4.1
2	53.0	1.92	11.8
3	2.9	1.50	3.8
4	5.4	1.27	2.8
5	5.9	0.66	1.4
6	52.0	2.61	2.2
Substrate	-	1.19	1.5

Table S2f. E = 0.52 V

Layer relative to surface	Thickness (Å)	Electron density ρ_e ($e^{-}Å^{-3}$)	Roughness (Å)
Electrolyte	-	0.38	-
1	96.6	1.11	5.4
2	15.6	1.06	3.5
3	11.3	1.25	3.8
4	8.5	0.83	2.8
5	6.1	0.51	1.4
6	52.2	2.61	2.2
Substrate	-	1.19	1.5

Table S2g. E = 0.37 V

Layer relative to surface	Thickness (Å)	Electron density ρ_e (e^-Å^{-3})	Roughness (Å)
Electrolyte	-	0.38	-
1	100.3	1.11	5.7
2	14.5	1.03	3.5
3	12.1	1.21	3.8
4	8.6	0.82	2.8
5	6.1	0.49	1.4
6	52.2	2.61	2.2
Substrate	-	1.19	1.5

The parameters determined from best fits to XRR data of Fig. 2A and used in Fig. 2B for the Ni (49.4 Å) / NiO (19.0 Å) bilayer film are given in Tables S3a-i.

Table S3a. E = 3.22 V (open circuit conditions)

Layer relative to surface	Thickness (Å)	Electron density ρ_e (e^-Å^{-3})	Roughness (Å)
Electrolyte	-	0.38	-
1	19.0	1.97	2.3
2	49.4	2.61	1.4
Substrate	-	1.19	1.5

Table S3b. E = 2.52 V

Layer relative to surface	Thickness (Å)	Electron density ρ_e ($e^{-}Å^{-3}$)	Roughness (Å)
Electrolyte	-	0.38	-
1	15.5	1.95	2.5
2	2.2	1.29	1.5
3	50.9	2.61	1.5
Substrate	-	1.19	1.5

Table S3c. E = 2.39 V

Layer relative to surface	Thickness (Å)	Electron density ρ_e ($e^{-}Å^{-3}$)	Roughness (Å)
Electrolyte	-	0.38	-
1	13.1	2.12	4.4
2	4.8	1.03	1.5
3	50.9	2.61	1.5
Substrate	-	1.19	1.5

Table S3d. E = 1.59 V

Layer relative to surface	Thickness (Å)	Electron density ρ_e ($e^{-}Å^{-3}$)	Roughness (Å)
Electrolyte	-	0.38	-
1	12.2	1.95	4.3
2	5.3	0.90	1.5
3	51.7	2.61	1.5

Substrate	-	1.19	1.5

Table S3e. E = 1.33 V

Layer relative to surface	Thickness (Å)	Electron density ρ_e ($e^-Å^{-3}$)	Roughness (Å)
Electrolyte	-	0.38	-
1	12.0	1.98	4.6
2	5.6	0.96	1.5
3	51.8	2.61	1.5
Substrate	-	1.19	1.5

Table S3f. E = 0.67 V

Layer relative to surface	Thickness (Å)	Electron density ρ_e ($e^-Å^{-3}$)	Roughness (Å)
Electrolyte	-	0.38	-
1	5.5	1.86	5.0
2	10.3	1.48	3.1
3	5.4	0.28	2.7
4	52.8	2.61	2.0
Substrate	-	1.19	1.5

Table S3g. E = 0.54 V

Layer relative to surface	Thickness (Å)	Electron density ρ_e ($e^-Å^{-3}$)	Roughness (Å)
Electrolyte	-	0.38	-
1	13.66	1.68	11.5
2	9.6	1.26	3.1

3	5.8	0.45	1.7
4	52.8	2.61	2.0
Substrate	-	1.19	1.5

Table S3h. E = 0.41 V

Layer relative to surface	Thickness (Å)	Electron density ρ_e ($e^{-}Å^{-3}$)	Roughness (Å)
Electrolyte	-	0.38	-
1	22.2	1.11	4.0
2	13.3	1.20	2.0
3	5.0	0.38	2.0
4	53.1	2.61	2.0
Substrate	-	1.19	1.5

Table S3i. E = 0.28 V

Layer relative to surface	Thickness (Å)	Electron density ρ_e ($e^{-}Å^{-3}$)	Roughness (Å)
Electrolyte	-	0.38	-
1	32.3	1.14	4.4
2	5.0	1.10	2.0
3	4.7	0.30	2.0
4	53.2	2.61	2.0
Substrate	-	1.19	1.5

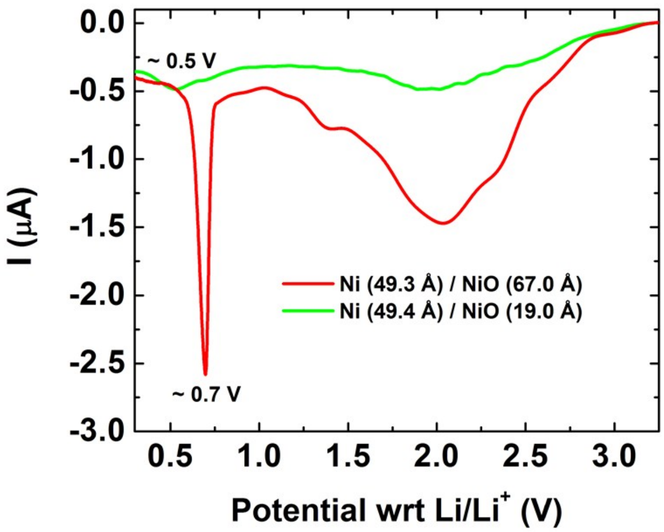

Fig. S1. The first discharge voltammograms for Ni (49.3 Å) / NiO (67.0 Å) and Ni (49.4 Å) / NiO (19.0 Å) electrodes (*operando* XRR measurements) measured at a voltage sweep rate of 0.1 mV s^{-1}. An abrupt onset of lithiation occurs near 0.7 V corresponding to the reduction of NiO to metallic Ni. A reductive peak near 2 V indicates formation of SEI layer and initial lithiation of NiO electrode.

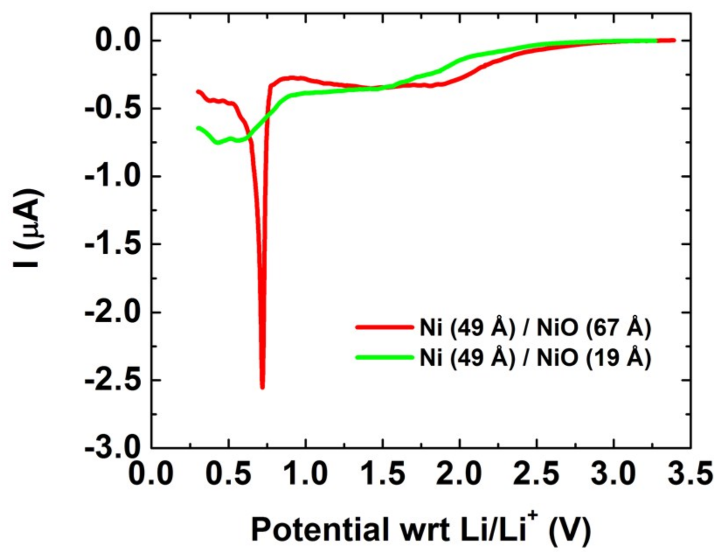

Fig. S2. The first discharge voltammograms for Ni (49.3 Å) / NiO (67.0 Å) and Ni (49.4 Å) / NiO (19.0 Å) electrodes (*operando* GISAXS measurements) measured at a voltage sweep rate of 0.1 mV s^{-1}.

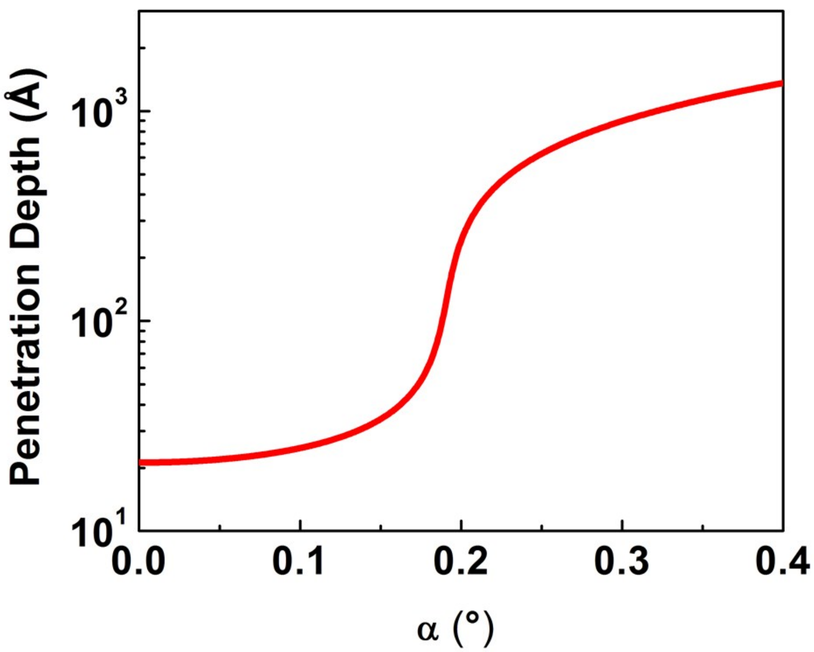

Fig. S3. Calculated penetration depth of X-rays at photon energy of E = 14.00 keV into NiO film immersed in electrolyte as a function of incident angle α. (Tolan, M., *X-ray scattering from soft-matter thin film: materials science and basic research*. Springer-Verlag: Berlin, 1999; Vol. 148, p. 10)

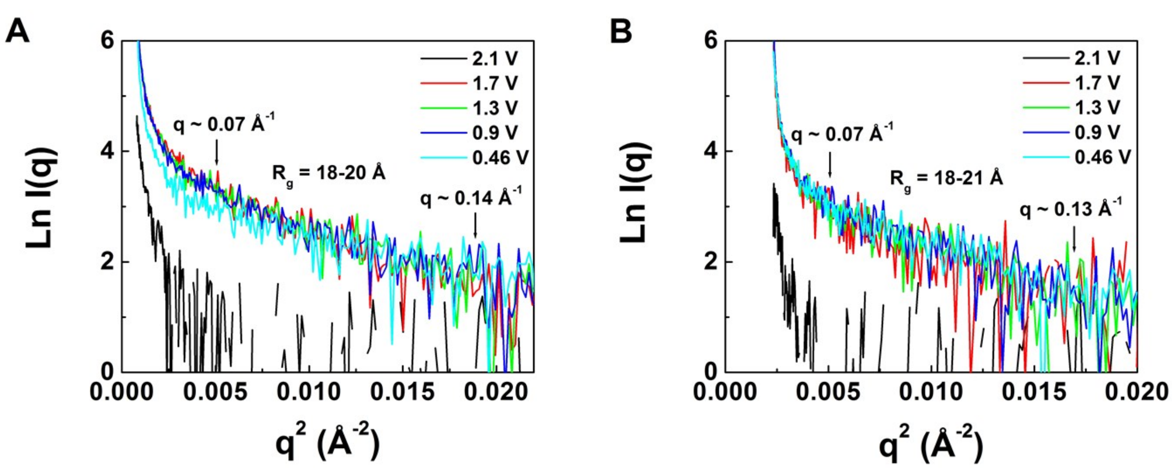

Fig. S4. Guinier plots of horizontal line cuts of 2D GISAXS patterns at different incident angles for the bilayer Ni (50 Å) / NiO (200 Å) electrode during lithiation: (A) α = 0.12°, (B) α = 0.20°.

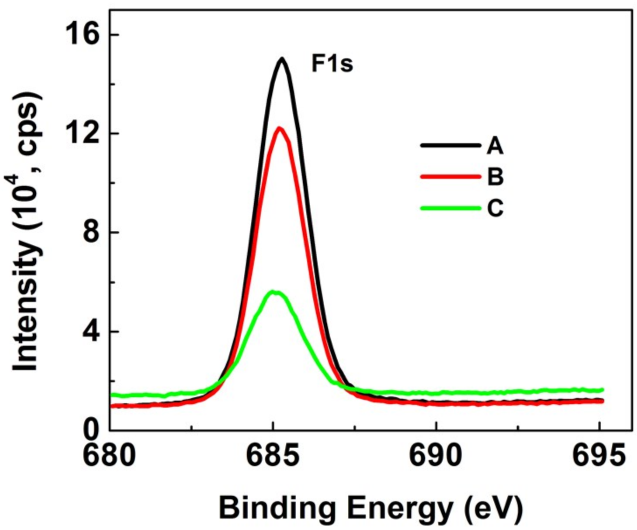

Fig. S5. F1s XPS spectra for the Ni (34 Å) / NiO (65 Å) bilayer electrode after the first discharge from OC (3.3 V) to 1.7 V at depth positions marked by arrows A, B, and C in Figure 5C.

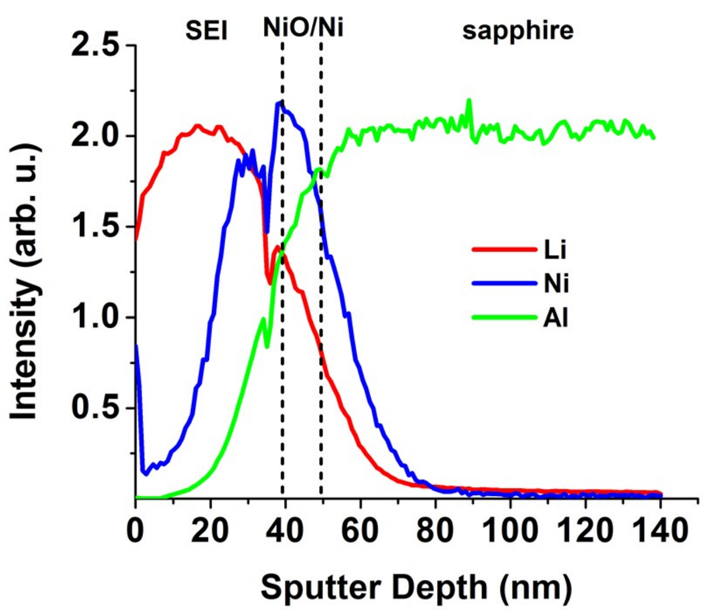

Fig. S6. ToF-SIMS depth profiles of Li, Ni and Al for the Ni (34 Å) / NiO (65 Å) bilayer film electrode after discharging from OC (3.3 V) to 1.7 V.

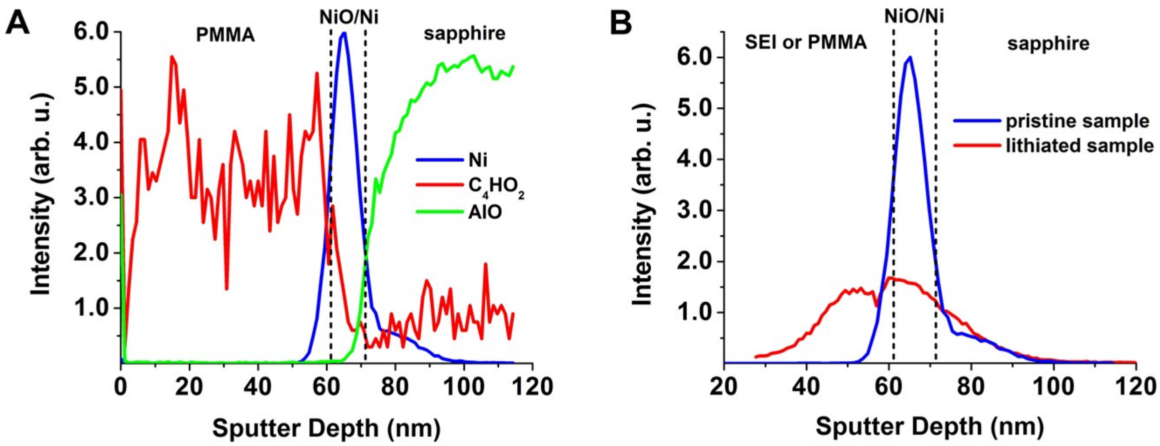

Fig. S7. (A) ToF-SIMS depth profiles for pristine Ni (34 Å) / NiO (65 Å) bilayer film spin-coated by PMMA (MW = 495 000). (B) Comparison of Ni depth profiles for pristine (with PMMA on the top) film and lithiated Ni/NiO bilayer film from Figure S6.

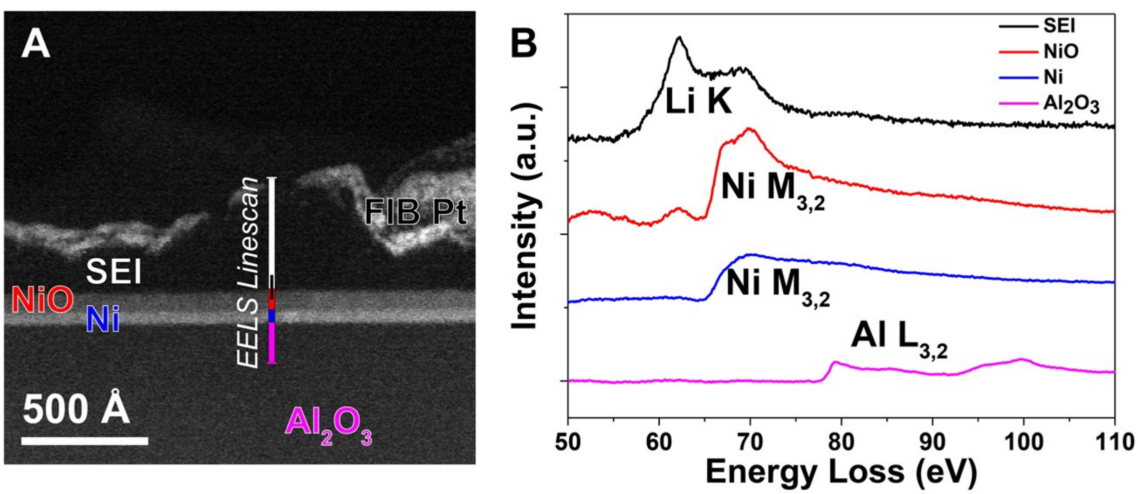

Fig. S8. A) High-angle annular dark-field (HAADF) STEM image of the Ni/NiO bilayer cross-section. The EELS linescan is marked by the multi-colored line. Each colored region denotes the integration boundaries for EELS spectra from SEI, NiO, Ni, and Al_2O_3 regions. The black line within the multi-colored line marks the region from where spectra shown in Figure 7 were collected. B) Integrated EELS spectra of the different film layer regions.